Acta Crystallographica Section B
Structural Science
ISSN 0108-7681

Single crystal structure and molecular dynamics analysis of a *myo*-inositol derivative

Jan Dillen,* Martin W. Bredenkamp and Mare-Loe Prinsloo

Department of Chemistry, University of Stellenbosch, Private Bag X1, Matieland 7602, South Africa

Correspondence e-mail: jlmd@maties.sun.ac.za

Received 18 January 2000
Accepted 6 April 2000

The crystal structure of 5-*O*-*tert*-butyldimethylsilyl-3,4-*O*-carbonyl-1,2-*O*-cyclohexylidene-2-oxo-3-oxa-4-bornanylcarbonyl-D-*myo*-inositol has been studied by single-crystal X-ray diffraction at both room temperature and 173 K. At room temperature, the *tert*-butyldimethylsilyl group exhibits dynamical disorder. A molecular dynamics simulation was used to model the disorder and this indicates that the group librates between two stable conformations in the crystal. Approximate relative energies of the different forms and energy barriers for the transition were obtained by empirical force field methods. Calculations of the thermal motion of the atoms are in good qualitative, but fair to poor quantitative agreement with the X-ray data.

1. Introduction

D-*myo*-Inositol-1,4,5-triphosphate (IP_3) is an important second messenger for the liberation of ribosomal calcium for the enhancement of cell metabolysis (Billington, 1993). D-*myo*-Inositol-1,3,4,5-tetraphosphate also enjoys considerable attention in research owing to its related metabolic activity. Despite the relative simplicity of these compounds, they pose a considerable challenge for synthesis because of the need for the selective phosphorylation of some of the six contiguous hydroxy groups. *myo*-Inositol has a plane of symmetry because only one of the hydroxy groups is axial. The problem of regioselectivity is thus compounded by a need for stereoselectivity. Sugar derivatives (Chen *et al.*, 1996) and quebrachitol (Akiyama *et al.*, 1990; Kozikowski *et al.*, 1994) have been used as chiral precursors. Alternatively, chirality has been induced by coupling an enantioselective chiral auxiliary

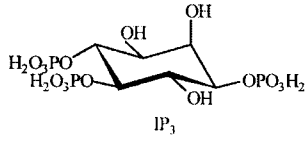

IP_3

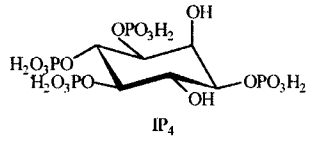

IP_4

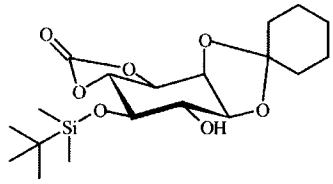

(1)

to *myo*-inositol (Pietruswicz *et al.*, 1992) or incorporated by adding a chiral auxiliary such as (*S*)-(−)-camphanic chloride to racemic *myo*-inositol derivatives and separating the resultant diastereomers. Camphanoates are often crystalline

and the diastereomers are usually separable chromatographically.

The value of tin-mediated selective derivatization of *myo*-inositol derivatives has not been fully explored. Of special interest are the selectivities that arise from contiguous equatorial hydroxy groups in the chair conformation of the cyclohexitol. We (Bredenkamp & Prinsloo, 2000) have used tin reagents to incorporate both the silyl and carbonate groups selectively. The differentially protected racemic *myo*-inositol derivative (1) was thus prepared with only the 6-position not protected. In view of the potential synthesis of IP_3 and IP_4, it was necessary to resolve the racemate. Position 6 was esterified with (*S*)-(−)-camphanic chloride, generating a diastereomeric mixture which was easily separable chromatographically. The more polar diastereomer was also easier to crystallize, yielding crystals suitable for single-crystal X-ray structure determination, which is reported herein.

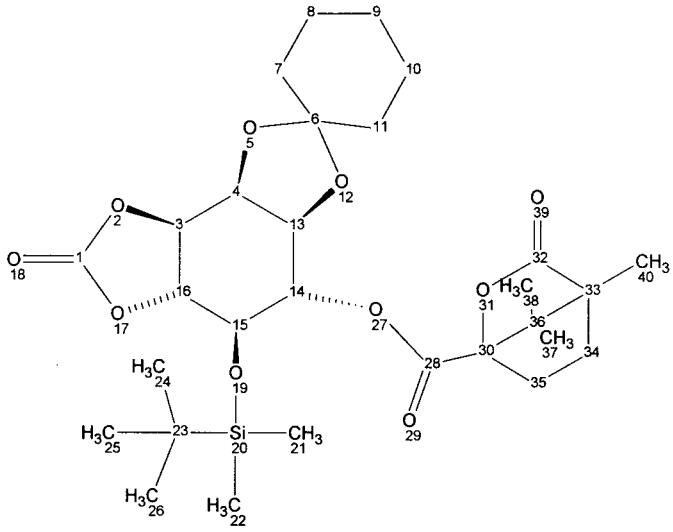

Figure 1
Schematic sketch of the structure, showing the atom numbering.

2. Experimental

A solution of the racemic penta-protected *myo*-inositol derivative (1) in dichloromethane together with a 10% catalytic amount of DMAP and an excess of triethylamine was treated with 20% excess (*S*)-(−)-camphanic chloride at 313 K for 3 h. The solvents were then removed and the residue separated with flash chromatography [SiO_2 pretreated with 2:7:93 Et_3N–EtOAc–petroleum spirits (333–353 K); stepped gradient from 5 to 100% EtOAc in petroleum spirits (333–353 K)], yielding equal amounts of the two diastereomers. The diastereomer with the smaller R_f value was crystallized from EtOAc/petroleum spirits (333–353 K; 34%) with m.p. 427–428 K. ^{1}H (300 MHz) and ^{13}C NMR (75 MHz) at 298 K in $CDCl_3$ (including APT, XHCORD and XHLR; Varian VXR 300) accounted for every proton and C atom, and was subtly different from the spectra of the diastereomer. Elemental analysis (University of Cape Town, South Africa): C 60.11, H 7.90%; $C_{29}H_{44}O_{10}Si$ requires C 59.98, H 7.64.

Details of the X-ray data collection are summarized in Table 1. Atom numbers are shown in Fig. 1. Atomic scattering factors were taken from the *International Tables for Crystallography* (1992, Vol. C). The structure was solved by direct methods (Sheldrick, 1990) and refined with the IRIX version of *SHELX*97 (Sheldrick, 1997). An unrestrained optimization resulted in unrealistic lengths for some of the bonds in the room-temperature structure and, therefore, all the Si—C bonds were restrained to the same value (σ = 0.005 Å) and also the C—C bonds in the *tert*-butyl group (σ = 0.01 Å). H atoms were placed on calculated positions. The known absolute configuration was confirmed by an absolute structure parameter (Flack, 1983) of x = 0.0 (2) calculated with the low-temperature data. The final coordinates and thermal factors of the non-H atoms are listed in Table 2.[1]

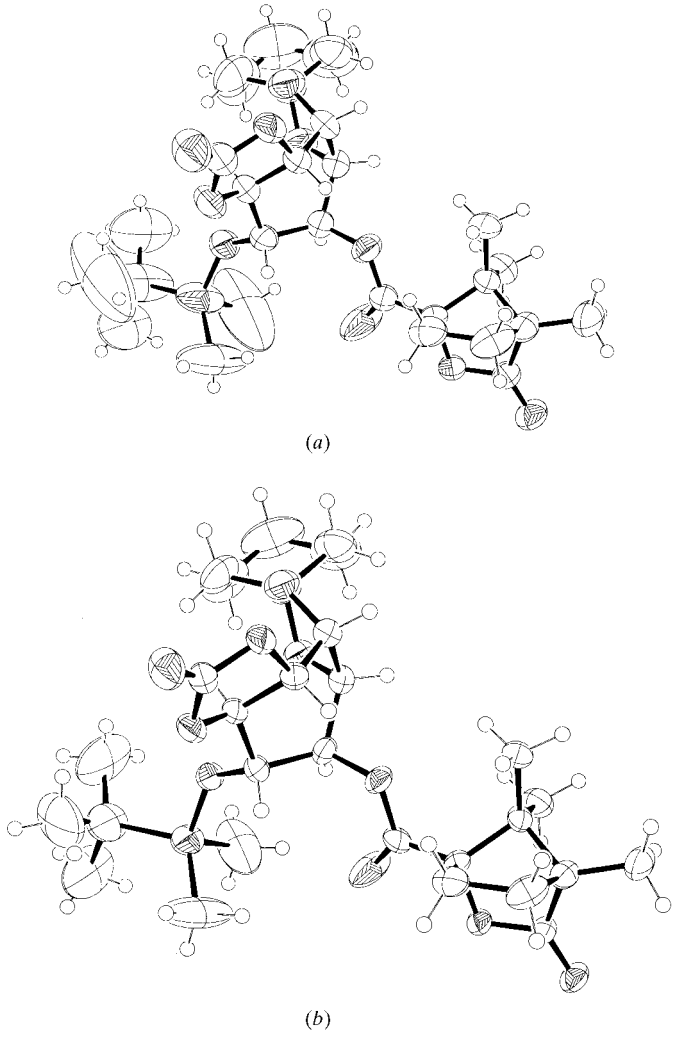

Figure 2
Perspective drawing of the experimental structures at (*a*) room temperature and (*b*) 173 K. Thermal ellipsoids are shown at the 50% probability level for the non-H atoms.

[1] Supplementary data for this paper are available from the IUCr electronic archives (Reference: NS0003). Services for accessing these data are described at the back of the journal.

Table 1
Experimental details.

	173 K	298 K
Crystal data		
Chemical formula	$C_{29}H_{44}O_{10}Si$	$C_{29}H_{44}O_{10}Si$
Chemical formula weight	580.73	580.73
Cell setting	Monoclinic	Monoclinic
Space group	$P2_1$	$P2_1$
a (Å)	7.537 (1)	7.5722 (4)
b (Å)	10.183 (1)	10.2402 (5)
c (Å)	20.843 (1)	21.1352 (9)
β (°)	94.93 (1)	96.188 (2)
V (Å^3)	1593.8 (3)	1629.29 (14)
Z	2	2
D_x (Mg m^{-3})	1.210	1.184
Radiation type	Mo $K\alpha$	Mo $K\alpha$
Wavelength (Å)	0.71070	0.71070
No. of reflections for cell parameters	6915	6199
θ range (°)	2.23–27.51	3.36–26.43
μ (mm^{-1})	0.125	0.122
Temperature (K)	173 (2)	298 (2)
Crystal form	Block	Block
Crystal size (mm)	0.20 × 0.15 × 0.13	0.5 × 0.4 × 0.3
Crystal colour	Colourless	Colourless
Data collection		
Diffractometer	Enraf–Nonius Kappa CCD	Enraf–Nonius Kappa CCD
Data collection method	A 175° ψ scan and 2 ω scans	A 175° ψ scan and 2 ω scans
Absorption correction	None	None
No. of measured reflections	6915	6439
No. of independent reflections	4237	6199
No. of observed reflections	3310	5230
Criterion for observed reflections	$I > 2\sigma(I)$	$I > 2\sigma(I)$
R_{int}	0.0292	0.0187
θ_{max} (°)	27.51	26.43
Range of h, k, l	$-8 \rightarrow h \rightarrow 9$ $-7 \rightarrow k \rightarrow 11$ $-23 \rightarrow l \rightarrow 23$	$0 \rightarrow h \rightarrow 9$ $-12 \rightarrow k \rightarrow 12$ $-26 \rightarrow l \rightarrow 26$
Refinement		
Refinement on	F^2	F^2
$R[F^2>2\sigma(F^2)]$	0.0513	0.0726
$wR(F^2)$	0.1281	0.1980
S	1.027	1.111
No. of reflections used in refinement	4237	6199
No. of parameters used	433	435
H-atom treatment	Mixed	Mixed
Weighting scheme	$w = 1/[\sigma^2(F_o^2) + (0.0643P)^2 + 0.7367P]$, where $P = (F_o^2 + 2F_c^2)/3$	$w = 1/[\sigma^2(F_o^2) + (0.0996P)^2 + 0.6765P]$, where $P = (F_o^2 + 2F_c^2)/3$
$(\Delta/\sigma)_{max}$	0.011	0.049
$\Delta\rho_{max}$ (e Å^{-3})	0.334	0.548
$\Delta\rho_{min}$ (e Å^{-3})	−0.304	−0.798
Extinction method	None	None
Source of atomic scattering factors	*International Tables for Crystallography* (1992, Vol. C, Tables 4.2.6.8 and 6.1.1.4)	*International Tables for Crystallography* (1992, Vol. C, Tables 4.2.6.8 and 6.1.1.4)
Computer programs		
Data collection	*Collect* (Nonius B. V., 1998)	*Collect* (Nonius B. V., 1998)
Data reduction	*Denzo–SMN* (Otwinowski & Minor, 1997)	*Denzo–SMN* (Otwinowski & Minor, 1997)
Structure solution	*SHELXS*97 (Sheldrick, 1990)	*SHELXS*97 (Sheldrick, 1990)
Structure refinement	*SHELXL*97 (Sheldrick, 1997)	*SHELXL*97 (Sheldrick, 1997)

3. Results and discussion

X-ray analysis of the room-temperature data reveals the disorder of the *tert*-butyldimethylsilyl (TBDMS) group and the large thermal movement of the atoms in the cyclohexane group. At 173 K the thermal motion of these atoms is still larger than for the rest of the molecule, but the structure is well resolved.

The slightly shorter C—C distances observed at room temperature in the cyclohexane ring average to a value of 1.519 Å, compared with 1.532 Å for the inositol ring, and may be explained by the libration of the atoms. However, it proved impossible to obtain a reasonable local geometry of the TBDMS group without the use of distance constraints, as explained above. In addition, as is evident from Fig. 2, least-squares minimization of the data results in excessively large temperature factors for the atoms involved.

Analysis of the Fourier maps did not allow a conclusive modelling of the observed disorder and, therefore, we undertook to study the crystal structure by molecular dynamics.

Calculations were performed with the *Cerius*[2] molecular modeling suite (Molecular Simulation Inc., 1998). Using the observed room-temperature coordinates as a starting point, the energy of the structure was first minimized within the context of the Universal Force Field (Rappé *et al.*, 1992) to obtain a good starting geometry for the subsequent simulation. Atomic charges were calculated with the charge equilibration method of Rappé & Goddard (1991). Molecular dynamics on the crystal were performed in $P1$ symmetry, using the NPT ensemble and a step size of 1 fs. Constant temperature was assured by coupling the molecular system to a constant heat bath using the T_Damping option, which applies dissipative Langevin forces to the atoms (Berendsen *et*

Table 2
Fractional atomic coordinates and equivalent isotropic displacement parameters (Å^2).

$$U_{eq} = (1/3)\Sigma_i\Sigma_j U^{ij} a^i a^j \mathbf{a}_i.\mathbf{a}_j.$$

	x	y	z	U_{eq}
T = 298 K				
C1	0.5376 (6)	0.8283 (4)	0.2125 (2)	0.0412 (11)
O2	0.3726 (3)	0.8806 (3)	0.21383 (13)	0.0388 (7)
C3	0.2486 (5)	0.7721 (4)	0.21512 (19)	0.0346 (9)
C4	0.0877 (5)	0.7939 (4)	0.25159 (19)	0.0387 (10)
O5	0.1396 (4)	0.8342 (3)	0.31560 (14)	0.0478 (8)
C6	0.0466 (6)	0.7549 (5)	0.3584 (2)	0.0501 (12)
C7	−0.1324 (7)	0.8161 (6)	0.3694 (3)	0.0702 (16)
C8	−0.2297 (9)	0.7332 (7)	0.4164 (4)	0.099 (2)
C9	−0.1145 (13)	0.7085 (8)	0.4789 (3)	0.122 (3)
C10	0.0632 (10)	0.6475 (7)	0.4660 (3)	0.100 (2)
C11	0.1609 (8)	0.7323 (6)	0.4212 (2)	0.0740 (17)
O12	0.0253 (4)	0.6324 (3)	0.32671 (13)	0.0437 (7)
C13	0.0001 (5)	0.6551 (4)	0.2593 (2)	0.0379 (10)
C14	0.0851 (5)	0.5387 (4)	0.22745 (18)	0.0361 (10)
C15	0.2936 (5)	0.5305 (4)	0.23423 (19)	0.0349 (10)
C16	0.3646 (5)	0.6677 (4)	0.2483 (2)	0.0329 (9)
O17	0.5365 (3)	0.6971 (3)	0.22414 (14)	0.0417 (7)
O18	0.6659 (4)	0.8887 (3)	0.20132 (16)	0.0573 (9)
O19	0.3526 (3)	0.4494 (3)	0.28583 (12)	0.0403 (7)
Si20	0.39989 (18)	0.29041 (13)	0.28804 (6)	0.0517 (4)
C21	0.4731 (13)	0.2360 (6)	0.2125 (3)	0.132 (4)
C22	0.1941 (9)	0.1977 (7)	0.3020 (5)	0.136 (3)
C23	0.5590 (9)	0.2701 (6)	0.3575 (3)	0.096 (2)
C24	0.5895 (14)	0.1220 (8)	0.3710 (4)	0.188 (6)
C25	0.4983 (13)	0.3345 (9)	0.4172 (3)	0.134 (3)
C26	0.7331 (9)	0.3442 (10)	0.3408 (6)	0.228 (7)
O27	0.0223 (3)	0.5502 (3)	0.15949 (13)	0.0379 (7)
C28	−0.0098 (5)	0.4380 (5)	0.1265 (2)	0.0433 (11)
O29	0.0191 (6)	0.3328 (4)	0.14909 (18)	0.0965 (16)
C30	−0.0844 (5)	0.4660 (4)	0.05944 (19)	0.0313 (9)
O31	−0.1429 (3)	0.3402 (2)	0.03029 (12)	0.0345 (7)
C32	−0.2592 (5)	0.3710 (4)	−0.02114 (18)	0.0320 (9)
C33	−0.2752 (5)	0.5170 (4)	−0.02418 (19)	0.0359 (10)
C34	−0.0892 (6)	0.5582 (5)	−0.0459 (2)	0.0533 (12)
C35	0.0419 (5)	0.5248 (4)	0.0126 (2)	0.0459 (12)
C36	−0.2534 (4)	0.5524 (4)	0.04849 (18)	0.0304 (9)
C37	−0.4073 (5)	0.5001 (4)	0.0850 (2)	0.0457 (12)
C38	−0.2265 (6)	0.6970 (4)	0.0627 (2)	0.0413 (11)
O39	−0.3239 (3)	0.2874 (3)	−0.05710 (13)	0.0412 (7)
C40	−0.4383 (7)	0.5672 (5)	−0.0645 (2)	0.0604 (14)
T = 173 K				
C1	0.5463 (5)	0.8249 (4)	0.2097 (2)	0.0655 (10)
O2	0.3830 (3)	0.8758 (2)	0.21123 (13)	0.0590 (6)
C3	0.2591 (4)	0.7685 (3)	0.21270 (18)	0.0515 (7)
C4	0.1003 (5)	0.7903 (4)	0.24825 (18)	0.0590 (9)
O5	0.1551 (4)	0.8332 (3)	0.31087 (15)	0.0748 (8)
C6	0.0617 (6)	0.7564 (5)	0.3535 (2)	0.0792 (13)
C7	−0.1121 (8)	0.8171 (7)	0.3641 (3)	0.106 (2)
C8	−0.2074 (13)	0.7366 (11)	0.4110 (5)	0.156 (4)
C9	−0.0855 (17)	0.7121 (13)	0.4725 (4)	0.193 (5)
C10	0.0842 (13)	0.6516 (12)	0.4599 (3)	0.157 (4)
C11	0.1822 (10)	0.7338 (9)	0.4148 (3)	0.120 (2)
O12	0.0401 (4)	0.6329 (3)	0.32271 (14)	0.0718 (7)
C13	0.0128 (5)	0.6547 (4)	0.25581 (17)	0.0569 (8)
C14	0.0976 (4)	0.5375 (4)	0.22527 (16)	0.0534 (8)
C15	0.3034 (4)	0.5284 (3)	0.23272 (16)	0.0506 (7)
C16	0.3755 (4)	0.6648 (3)	0.24568 (17)	0.0512 (8)
O17	0.5461 (3)	0.6937 (3)	0.22228 (14)	0.0648 (7)
O18	0.6728 (4)	0.8837 (3)	0.19854 (19)	0.0860 (10)
O19	0.3622 (4)	0.4481 (3)	0.28416 (12)	0.0633 (7)
Si20	0.4279 (3)	0.29636 (16)	0.28631 (7)	0.1166 (7)
C21	0.4766 (19)	0.2334 (8)	0.2127 (3)	0.205 (7)
C22	0.2297 (13)	0.2017 (11)	0.2936 (12)	0.43 (2)
C23	0.5605 (16)	0.2660 (8)	0.3581 (3)	0.252 (9)
C24	0.5776 (19)	0.1140 (9)	0.3705 (5)	0.203 (6)
C25	0.4790 (19)	0.3250 (12)	0.4167 (3)	0.205 (6)
C26	0.7268 (15)	0.3513 (17)	0.3384 (13)	0.57 (3)
O27	0.0327 (3)	0.5484 (3)	0.15776 (12)	0.0594 (6)
C28	−0.0094 (5)	0.4382 (4)	0.12628 (19)	0.0616 (9)
O29	0.0141 (8)	0.3343 (4)	0.1486 (2)	0.138 (2)
C30	−0.0833 (4)	0.4665 (3)	0.05901 (16)	0.0479 (7)
O31	−0.1426 (3)	0.3419 (2)	0.03012 (11)	0.0512 (5)
C32	−0.2589 (4)	0.3723 (3)	−0.02149 (16)	0.0494 (7)
C33	−0.2732 (5)	0.5188 (4)	−0.02458 (17)	0.0563 (8)
C34	−0.0874 (7)	0.5569 (5)	−0.0450 (2)	0.0768 (12)
C35	0.0430 (5)	0.5236 (5)	0.0141 (2)	0.0696 (11)
C36	−0.2515 (4)	0.5522 (3)	0.04784 (15)	0.0468 (7)
C37	−0.4049 (5)	0.5008 (5)	0.0824 (2)	0.0680 (10)
C38	−0.2234 (6)	0.6969 (4)	0.0617 (2)	0.0640 (10)
O39	−0.3236 (4)	0.2899 (3)	−0.05682 (13)	0.0653 (7)
C40	−0.4371 (8)	0.5681 (5)	−0.0654 (2)	0.0889 (15)

al., 1984). After an initial 5 ps of equilibration, data for the simulation was collected over a system time of 1 ns at a temperature of 300 K. Ewald summations were performed for both the van der Waals and the electrostatic interactions. As evident from Table 3, despite the reduction of the symmetry to *P*1 for the purposes of the calculations, on average, the crystal remains monoclinic.

Analysis of the generated trajectory shows that during the simulation, the torsion angle C15—O—Si—C23 of both molecules in the unit cell changes repeatedly between a value of approximately −130 to +160°, as illustrated in Fig. 3. This suggests that the disorder observed in the crystal is dynamic, rather than static in nature. Since the calculations were performed in *P*1 symmetry, the predicted existence of two possible molecular conformations results in three distinct crystals to be considered for discussion. In addition to the torsion angle above, the two conformations differ in a number of other features, of which a rotation of the *tert*-butyl group of

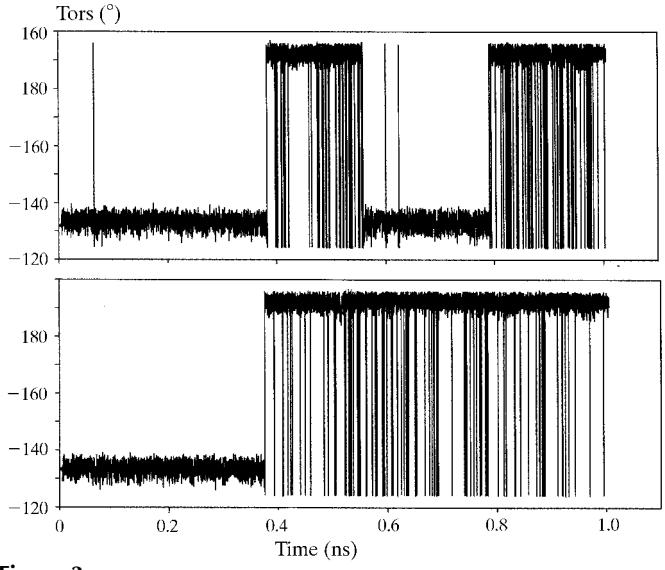

Figure 3
Profile of the C15—O—Si—C23 torsion angle for both molecules during the molecular dynamics run. Configurations were noted every 10 fs.

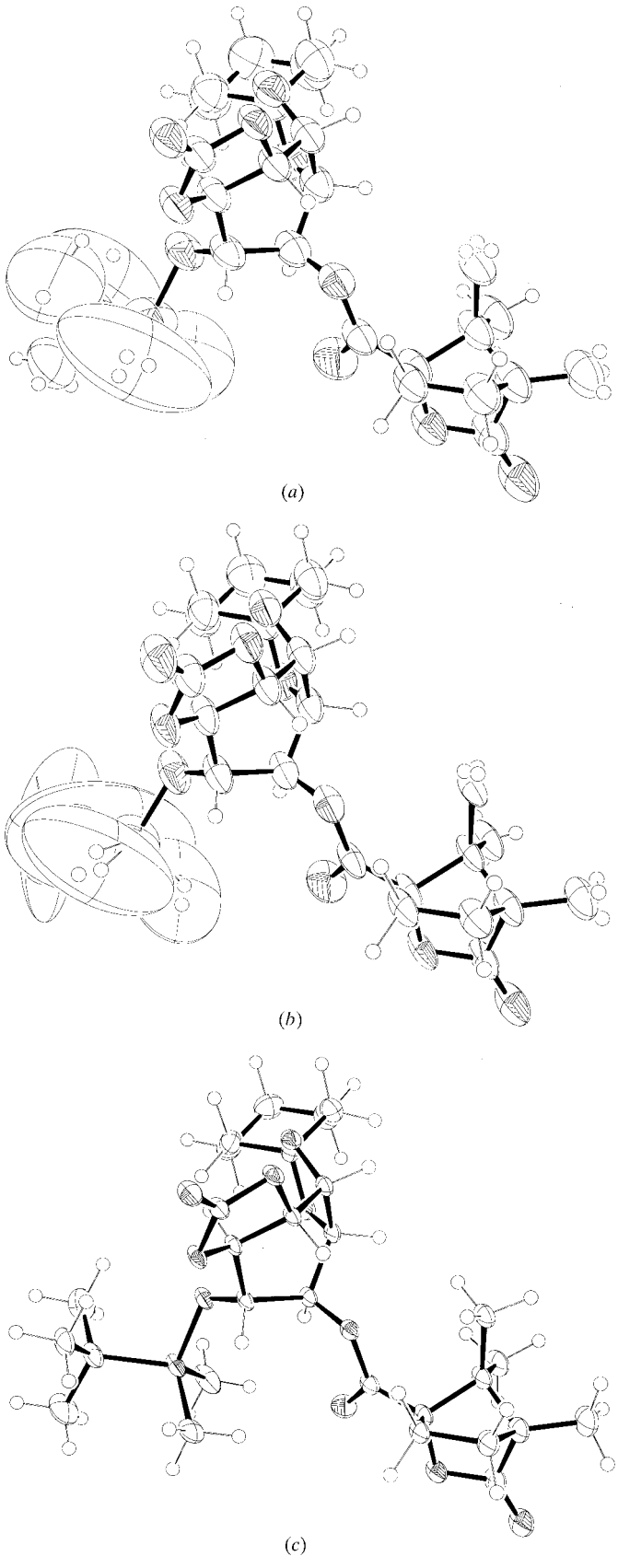

Figure 4
Calculated thermal ellipsoids for both molecules at (*a*) room temperature and (*b*) for one molecule at 175 K. The disorder in the TBDMS group is very evident in the former.

~20° and a change in the C16—C15—O—Si torsion angle by the same amount are the most prominent. However, for the purposes of discussion, only the difference in C15—O—Si—C23 will be considered.

The calculated structure most closely related to the experimental one has the crystallographically observed $P2_1$ symmetry. If we denote the conformation of this structure as *AA*, then a change in the conformation of one of the molecules results in *AB*, which is calculated to have *P*1 symmetry. If both molecules are in the alternative conformation, the resulting *BB* structure again has $P2_1$ symmetry. All three forms are minimal in the energy hypersurface, as shown by the correct number of vibrational frequencies, with relative energies as given in Table 4 under model I. Surprisingly, the calculations predict that the *BB* form is the most stable conformation, albeit only by 4.2 kJ mol^{-1}, in contradiction with the findings of the low-temperature study, whose structure resembles more closely the calculated *AA* form.

Clearly, these results indicate either a deficiency in the force field employed or in the way the calculations are performed. Since the molecule under study does not contain any 'unusual' atoms for which the force field may be ill-parameterized, the computational model was investigated first.

The process of calculating the energy of a three-dimensional periodic system involves, apart from calculating the intramolecular interactions, a summation of the energy terms between all the atoms in the central unit cell and all the surrounding cells. In this process, it is assumed that all these surrounding cells are exact copies of the central cell. Since we are dealing with a disordered crystal, the validity of this picture breaks down as it is exactly the experimental observation of the disorder which demonstrates that the unit cells are not identical in the macroscopic crystal. Thus, the results in Table 4 are for *all* unit cells in either *AA*, *AB* or *BB* and hence ignore the fact that there is disorder. This poses a problem for a more physically correct calculation of the energy as it is not clear in advance what the relative abundance is of unit cells with molecules in any of these conformations.

To reduce the amount of computational effort, it was decided to calculate the relative energies of the conformations using a model with maximal relative disorder, *i.e.* a disordered unit cell surrounded by ordered cells, the reasoning being that both models may then be viewed as the upper and lower limit of the actual situation. Thus, a unit cell consisting of the original crystallographic unit cell, surrounded by molecules to form a new 3 × 3 × 1 block of unit cells was created. Expansion of the system along the *c* axis was omitted because of the larger dimension of this axis. The resulting block was then considered to be the new unit cell of the crystal and calculations were performed as above. Relative energies of the different crystals were obtained by changing the conformations of the molecules in what was the original central unit cell only, leaving the surrounding cells in their original form and minimizing the energy of the complete system. The physical picture is thus that of a molecule that changes conformation, surrounded by one layer of unit cells where the molecules do not change. Energy values are given in Table 4 under model II

Table 3
Average calculated cell parameters.

Parameter	175 K	300 K
a (Å)	7.6 (1)	7.59 (1)
b (Å)	10.05 (7)	10.14 (12)
c (Å)	20.95 (22)	21.2 (3)
α (°)	90.0 (14)	90.2 (19)
β (°)	92.6 (9)	94.6 (19)
γ (°)	90.0 (9)	90.2 (13)

Table 4
Relative energies (kJ mol^{-1}) of the calculated crystal structures.

Conformation	Space group symmetry	ΔE Model I	ΔE Model II
AA	$P2_1$	0.0	0.0
AB	$P1$	−1.3	12.2
BB	$P2_1$	−4.2	21.8

and may be interpreted as the upper limit in energy difference between the different forms to be considered. As can be seen from Table 4, the values are quite different from the values obtained with model I and are, in view of the crystal structure obtained at 173 K, probably much too high. Model II was also used to calculate the energy barriers for the conformational conversion. These were obtained by driving the C15—O—Si—C23 torsion angle in steps of 5°, while forcing the *tert*-butyl group and the C16—C15—O—Si angle to change simultaneously by a small amount, followed by an energy minimization at a fixed value of the C15—O—Si—C23 angle. Restraining these two additional angles proved necessary to force the conformation from *A* to *B* and *vice versa*. The calculations indicate that the total net barrier for a transition from the *AA* to the *BB* form is ∼25.1 kJ mol^{-1}.

Calculations of the temperature factors from the trajectory generated during the dynamics run show a picture that is qualitatively in agreement with the results from X-ray diffraction. The simulation at 300 K produces very large thermal motion for the atoms in both the TBDMS group and the cyclohexane group, as observed by experiment. The poor numerical agreement in anisotropy, especially if the results for the two independent molecules in Fig. 4 are compared, may be the result of a simulation time which is too short. The thermal ellipsoids also seem to suggest a net translation of the molecules in the *P*1 unit cell during the simulation. Despite these shortcomings, the calculations correctly predict the higher thermal motion of the atoms in the cyclohexane ring, which in the crystal is in relatively close contact to the disordered TBDMS group and thus is likely to exhibit this behaviour.

The X-ray data were also investigated in terms of the two stable conformations identified by the calculations. A static disorder model consisting of the TBDMS in the two possible orientations using isotropic temperature factors for the atoms involved and the same restraints as above refined to R = 0.1045 (wR = 0.2633) for 433 variables. The geometry of the resulting fragments showed some non-physical distortions, especially the valence angles.

The molecular dynamics calculations on the title compound were repeated at 175 K for the same simulation time of 1 ns and these predict that at this temperature, no conformational changes similar to those observed at room temperature are to be expected. However, experimental thermal motions of some atoms in the TBDMS group are in excess of the average compared with other regions of the molecule. A static disorder model with isotropic temperature factors and distance constraints as above refined to R = 0.0534, compared with R = 0.0517 for the standard refinement. Despite the higher residual, this model warrants some discussion as the valence angles of the fragments have meaningful values. The two fragments differ by a C15—O—Si—C23 torsion angle of ∼16° and a rotation of the *tert*-butyl group of 10°. Refinement proceeds to a 45–55% abundance ratio. For comparison, the calculated s.u. for the C15—O—Si—C23 torsion angle is 6.6° and the s.u. for the rotation of the *tert*-butyl group 6.9°. The calculated temperature factors are also smaller than found experimentally and it thus appears that the experimental structure at 173 K may be partially disordered, but this is not supported by the calculation.

References

Akiyama, T., Takechi, N. & Ozaki, S. (1990). *Tetrahedron Lett.* **31**, 1433–1434.

Berendsen, H. J. C., Postma, J. P. M., van Gunsteren, W. F., DiNola, A. & Haak, J. R. (1984). *J. Chem. Phys.* **81**, 3684–3690.

Billington, D. C. (1993). *The Inositol Phosphates. Chemical Synthesis and Biological Significance.* New York: VCH Publishers.

Bredenkamp, M. W. & Prinsloo, M.-L. (2000). To be published.

Chen, J., Dormán, G. & Prestwich, G. D. (1996). *J. Org. Chem.* **61**, 393–397.

Flack, H. D. (1983). *Acta Cryst.* A**39**, 876–881.

Kozikowski, A. P., Fauq, A. H., Wilcox, R. A. & Nahorski, S. R. (1994). *J. Org. Chem.* **59**, 2279–2281.

Molecular Simulations Inc. (1998). *Cerius*^{2}, Release 3.8. San Diego, USA.

Nonius B. V. (1998). *Collect*. Delft, The Netherlands.

Otwinowski, Z. & Minor, W. (1997), *Processing of X-ray Diffraction Data Collected in Oscillation Mode. Methods in Enzymology*, Vol. 276, *Macromolecular Crystallography*, Part A, edited by C. W. Carter Jr and R. M. Sweet, pp. 307–326. New York: Academic Press.

Pietruswicz, K. M., Salamoñczyk, G. M. & Bruzik, K. S. (1992). *Tetrahedron*, **48**, 5523–5542.

Rappé, A. K., Casewit, C. J., Colwell, K. S., Goddard III, W. A. & Skiff, W. M. (1992). *J. Am. Chem. Soc.* **114**, 10024–10035.

Rappé, A. K. & Goddard III, W. A. (1991). *J. Phys. Chem.* **95**, 3358–3363.

Sheldrick, G. M. (1990). *Acta Cryst.* A**46**, 467–473.

Sheldrick, G. M. (1997). *SHELX*97, Version 97–2. University of Göttingen, Germany.